**Tree and stand characteristics associated with the occurrence of false heartwood in individual Japanese white birch trees**

Akira Nakaya[1*], Hisashi Osaki[2], Yasuyuki Ohno[3], Toshiya Yoshida[1]

[1]Field Science Center for Northern Biosphere, Hokkaido University, Nayoro, Japan

[2]Hokkaido Forest Products Research Institute, Asahikawa, Japan

[3]Hokkaido Forestry Research Institute, Bibai, Japan

***Corresponding author**

Akira Nakaya

E-mail: nakaya.akira.o8@elms.hokudai.ac.jp

**Abstract**

New wood uses of Japanese white birch (*Betula platyphylla* var. *japonica*) have attracted much attention in recent years, but false heartwood has led to a decline in commercial value due to its irregular wood color. In this study, we assessed the occurrence of false heartwood and its proportion to stem cross-sectional area (PFH) in individual Japanese white birch (482 trees) in a ca. 70-year-old natural secondary forest. Specifically, we investigated the relative strength of the direct/indirect effects of individual size (BA), growth rate (GR), crown ratio (CR), number of branch scars (NBS), basal area sum of neighboring trees (BAS) and topographic wetness index (TWI) on PFH. In total, 80.3% of trees had false heartwood. CR was found to be the most important factor, acting through direct and indirect negative effects. BA and NBS had a positive effect, and TWI had a negative effect on PFH. BA had a positive correlation with tree age, indicating that PFH can be reduced in trees with faster growth. Simultaneously, BAS had an indirect positive effect on PFH. These results suggested that thinning, which reduces BAS and increases CR, can reduce false heartwood.

**Keywords:** *Betula platyphylla*; wood discoloration; wood properties; structural equation modeling; standing tree characteristics

**Introduction**

False heartwood (also called red heartwood) is defined as the central part of wood, with a different nuance of color than surrounding normal wood, in tree species that normally do not have any heartwood (Venet, 1986; Hörnfeldt et al., 2010). The conditions for its occurrence and formation process have been studied in beech (*Fagus*), maple (*Acer*), and birch (*Betula*) species (Campbell and Davidson, 1941; Shigo, 1984; Hallaksela and Niemistö, 1998; Wernsdörfer et al., 2005; Giroud et al., 2008; Havreljuk et al., 2013). The first step in the formation process is the penetration of oxygen and microorganisms into the wood from damaged areas of the stem, such as fallen branches (Trendelenburg, 1939; Shigo, 1986; Kohler, 2006; Belleville et al., 2011). In subsequent stages, especially when tree vigor is weak, under dry conditions (Shigo, 1986; Kohler, 2006), the oxidation of phenolic substances (Koch, 2004; Hofmann et al., 2022) and enzymes released by fungi (Trendelenburg, 1939; Pape, 2002) may expand discoloration in the stem.

In general, the commercial value of wood containing false heartwood is significantly reduced since irregular coloring is not attractive to many consumers. Therefore, previous studies have attempted to predict the presence or absence of false heartwood and its proportion to stem cross-sectional area based on tree appearance characteristics (Knoke and Wenderoth, 2001; Račko and Čunderlík, 2002, 2010; Wernsdörfer et al., 2005; Belleville et al., 2011; Baral et al., 2013). Several studies have stated that the development of false heartwood is related to age, suggesting that it may be possible to produce wood with less false heartwood by accelerating growth to shorten the time to harvest (Hallaksela and Niemistö, 1998, Knoke, 2003; Giroud et al., 2008; Drouin et al., 2009; Baral et al., 2013). Kohler (2006), on the other hand, emphasized that a combination of factors leads to the formation of false heartwood and that the most important factor influencing its formation is the growth environment of the stand, including stand density. Furthermore, Giroud et al. (2021) demonstrated the importance of topography and moisture conditions; dryness conditions contributed to increasing the proportion of false heartwood in white birch (*Betula papyrifera* Marsh.). However, although one study examined multiple factors in an integrated manner (Belleville et al., 2011), the relative importance of each factor is not clear. Furthermore, the decline in commercial value is also due to the difficulty in distinguishing between false heartwood and decayed wood (Kohler, 2006). False heartwood without decay has been reported to have higher moisture content and more abundant fungi than normal wood (Campbell and Davidson, 1941), but the difference in the mechanical properties (strength and hardness) was unclear. Nevertheless, false heartwood and decay are thought to be related (Trendelenburg, 1939; Campbell and Davidson, 1941; Siegle, 1967; Shigo and Hillis, 1973; Basham, 1991; Arač et al., 2021). Stem damage, which is considered to be the starting point of false heartwood formation can also be an entry point for heart rot fungi (Trendelenburg, 1939).

Japanese white birch (*Betula platyphylla* Sukaczev var. *japonica* (Miq.) H. Hara) trees grow quickly with a potential life span of approximately 100 years (Osumi, 2005), and their high reliability of natural regeneration (Aoyama et al., 2009; Yamazaki and Yoshida, 2018) makes planning for sustainable wood use easy. The wood of this species has been used only for low-quality applications, such as pulpwood, but the development of processing technology has made it possible to efficiently use logs even with small diameters for high value-added items, such as furniture and interior materials (Shimase, 2021). To promote the use of Japanese white birch for a wider variety of applications, it is necessary to understand the basic characteristics of false heartwood, such as its frequency of occurrence, requirement for formation, and relationship to decay incidence. This study aims to verify the following hypotheses about the proportion of false heartwood (PFH), and its relationship with decay, in individual Japanese white birch grown in a relatively old (approximately 70 years old) secondary stand; higher PFH is associated with (1) a lower crown ratio, (2) a greater number of branch scars, (3) a greater individual tree basal area, (4) a lower growth rate, (5) lower topical moisture conditions (wetness) surrounding the tree, and (6) occurrence of decay.

This study also addresses the vertical distribution of false heartwood within the tree stem. Several studies have shown that the size of false heartwood varies with vertical tree stem position (Hallaksela and Niinistö, 1998; Wernsdörfer et al., 2006; Giroud et al., 2008; Baral et al., 2013) and that false heartwood is mostly located under the lowest live branch (Basham, 1991; Belleville et al., 2011; Giroud et al., 2008). According to Wernsdörfer et al. (2006), there are three stages of false heartwood development, which are thought to proceed in the following order: false heartwood initiation, a transition stage in which false heartwood develops especially at the middle stem height, thus showing a vertically spindle shape, and a late stage in which false heartwood becomes vertically conical along the stem. Therefore, the following hypotheses are also tested in this study; false heartwood (7) occurred only under the lowest live branch, and (8) shows a vertically conical shape, considering that the age of the study stand is close to the maturity.

## Materials and methods

### *Study site and sampling*

Field surveys were conducted in the Uryu Experimental Forest, Field Science Center for Northern Biosphere, Hokkaido University, Japan (44°22′ N, 142°12′ E, 280 m above sea level). The mean annual temperature and precipitation in the forest are 6.0 °C and 1,500 mm, respectively, according to the Japan Meteorological Agency (https://www.jma.go.jp/jma/index.html). The maximum snow depth reaches more than 200 cm. The dominant vegetation is natural mixed forest consisting of cool temperate hardwood and subboreal conifer species. In addition, there are natural secondary forests dominated by *Betula* spp.

From January to April 2020 and 2021, experimental cutting was conducted in a ca. 70-year-old natural secondary forest, which was located on the upper slope (prone to dryness) from the lower slope. This forest was crowded in terms of tree density (546 stems·ha$^{-1}$), as it was established without human interference (such as thinning) after field burning in approximately 1950. Three clear-cut plots (two plots of 1.09 and 0.99 ha cut in 2020, one plot of 1.09 ha cut in 2021) were set as the study area. *B. platyphylla* overwhelmingly dominated the study area (69% in volume, 69% in basal area, 65% in stem density), with *Quercus crispula* Blume, *Betula ermanii* Cham, *Abies sachalinensis* (F. Schmidt.) Mast., as occasional associates (Table 1). The understory was densely covered with *Sasa senanensis* (Franch. et Sav.) Rehder.

***Methods***

Tree measurements were conducted one year before each cutting (April 2019 and 2020). All living trees with a diameter at breast height (DBH; 1.3 m above ground) greater than 12 cm were numbered with tags for individual identification. Their DBH was measured in 2 cm intervals with a caliper, and location (x-y coordinates) was recorded by GPS (Mobile Mapper 100, Ashtech). In addition, photographs of each standing tree were taken (Camera; D 750, Nikon Co., Lens; AF-S NIKKOR 18-35 mm f/3.5-4.5 G ED, Nikon Co.) at the time of complete defoliation (December-February) from two points facing each other at approximately more than 10 m away from the stem so that the breast height to the crown top was captured with small lens distortion.

The trees were felled with a chainsaw at an average height of 0.67 (s.d. 0.16) m above the ground. After transporting the log to the stock yard using a heavy machine while retaining the individual identification number, disks with 5 cm thickness were collected from the butt end of the log (951 disks). The existence of decay on the butt end of the log (cross section) was also recorded mainly by visual inspection. If it was difficult to judge by visual inspection alone, it was determined to be decaying when the material easily crumbled by scratching with a tool.

The disks were brought back to the lab and the cross sections were photographed along with a scale (Camera; D 750, Nikon Co., Lens; AF-S NIKKOR 18-35 mm f/3.5-4.5 G ED, Nikon Co.). The periphery of the surface area (excluding the bark) and false heartwood were manually delineated in ImageJ (Schneider et al., 2012), and the respective areas were measured. Here, false heartwood is defined as “wood with a different nuance of color from surrounding wood” (Venet, 1986), and the proportion of false heartwood (PFH) was calculated as the proportion to the disk surface area. The ring widths for the last 10 years were also measured from the cambium to one direction (which represents average growth), and the cross-sectional area growth rate (for the last 10 years) was calculated based on the ratio of distance (radius) to the pith (GR). In addition, we randomly selected 100 disk photographs and counted the number of these annual rings. The possibility of counting false annual rings was minimized by enlarging the image data.

The photographs of individual standing trees taken during the complete defoliation season (see above) enabled us to record tree form and stem characteristics. First, the crown ratio (CR; the ratio of crown length to tree height) was recorded. In this study, the ratio of crown length to tree height was read directly on standing tree photographs at a resolution of 10%. Here, the crown refers to the area where the live branches are continuous up to the shoot ends from the lowest live branch. Next, branch scars (Figure 1) located from breast height to the bottom of the lowest living branch were counted by using the two images taken from opposite positions; those with a width greater than 1/3 of the stem diameter at the height were targeted. The number of branch scars (NBS) was measured with accuracy by enlarging the photographs and paying attention to the position and characteristics of individual branch scars to avoid omissions and duplicates in the count. In these steps, the trees (469/951 individuals) that were difficult to discriminate due to overlapping stems or branches of other trees were excluded from the analysis.

As an indicator of local tree crowding, we calculated the total basal area of living trees with a diameter at breast height (DBH) of 12 cm or more within a 5-meter radius from the study tree (i.e., amounts of neighboring trees; BAS). This radius corresponds to the maximum crown radius of trees in the study site. We used GIS software (QGIS: QGIS Development Team, 2021) and the location information (x-y coordinates) of trees for the calculation. Then, a numerical topographic map was overlaid on the GIS (QGIS), and the slope inclination was calculated at 400 $m^2$ resolution to obtain the topographic wetness index, which is a relative indicator of the topical wettability of all individuals (TWI: Beven and Kirkby, 1979).

In addition, 32 randomly selected birch trees (DBH = 23.8 (s.d. 2.0) cm) in the study area were felled to investigate the vertical distribution of false heartwood. Their stump height, whole tree height and lowest live branch height (defined as the branching height of the lowest foliage layer forming a contiguous living canopy) were measured. Subsequently, disks of 5 cm thickness were collected from these trees at the stump height, 1 m, 1.3 m, 2 m, and then every 1 m to the treetop. All disks were brought back to the lab, and PFH was measured on each disk photograph as described above. The false heartwood volume of the entire tree was then calculated as follows:

[1] $$FHVlog = \left(\frac{FHT+FHB}{2}\right) \times \log length$$

[2] $$FHV = \sum^{n} FHVlog$$

where FHVlog is the false heartwood volume per log ($m^3$), FHV is the false heartwood volume of the entire tree ($m^3$), FHT is the surface area of false heartwood for the top end ($m^2$), and FHB is the surface area of false heartwood for the butt end ($m^2$) (Giroud et al. 2008). FHV was converted to PFHV, which is the proportion of false heartwood volume to entire stem volume.

***Analysis***

We performed structural equation modeling (SEM) to determine the strength of the direct and indirect effects of each factor on the proportion of false heartwood (PFH). A hypothetical model (Figure 2) was developed that accounted for previous studies. Based on the mechanism of false heartwood formation, we hypothesized that basal area (BA) and number of branch scars (NBS) would have a positive direct effect. Similarly, we hypothesized that the growth rate (GR), crown ratio (CR), and TWI had a negative direct effect on PFH. For indirect effects, the paths were assumed to indicate that BA affects PFH indirectly by affecting GR, CR, and NBS. Since CR could affect NBS and GR, TWI could affect PFH via GR, and indirect paths from these two variables were also assumed. Regarding the amounts of neighboring trees (BAS), only indirect paths through BA, NBS, CR, and GR were assumed. SEM analyzes the relationship between hypothesized variables in the form of a linear combination (Lam and Maguire, 2012). Hence, we examined the bivariate relationships using simple linear regression analysis according to the hypothesis in Figure 2, and the assumption of linearities was satisfied for the variables between which we assumed a causal relationship. Normality for each variable was confirmed at $P > 0.05$ based on the Shapiro–Wilk test (Razali and Wah, 2011). For all unstandardized path coefficients, the significance level was set at a risk rate of less than 5%. However, SEM is a statistical method used to test a theoretical hypothesis. Therefore, nonsignificant paths were retained in the model if prior studies showed a significant relationship or if they were conceivable theoretically valid (Laughlin and Fulé, 2008; Lam and Maguire, 2012).

The model fit was evaluated by the goodness-of-fit index (GFI), adjusted goodness-of-fit index (AGFI), comparative fit index (CFI) and root mean square error of approximation (RMSEA). The values of GFI, AGFI and CFI range between 0 and 1, and the better the model is, the closer the value is to 1. RMSEA values between 0.05 and 0.08 indicate an adequate fit. The SEM was analyzed using the “lavaan” (Rossel, 2012) package in R version 4.1.3 (R Development Core Team, 2022).

The relationship between false heartwood and decay was tested using the chi-square test for differences in the proportion of false heartwood occurrence in all study trees and trees with decay. In addition, to determine if there were differences in the proportion of decay depending on PFH, all trees were classified into the following PFH classes: PFH = 0, 1-10, 11-20, or PFH ≥ 21%. Then, a chi-square test was performed, and an adjustment for multiple comparisons was made using Tukey’s method when overall differences were found.

This study also investigated the vertical distribution of false heartwood (i.e., shape and relationship with the lowest live branch height) in individual trees. The relationship of the proportion of false heartwood volume to entire tree stem volume (PFHV) with PFH at relatively low tree height positions (stump, 1 m, 1.3 m, 2 m, and 3 m) was analyzed using

Pearson's correlation coefficient.

## Results

Among the 482 investigated trees in this study, false heartwood was found in 387 trees (80.3%). The proportion of individuals with PFH ≥ 11% reached 45.9% (Figure 3). The average PFH was 16.4 (s.d. 14.0) %, with a maximum of 63.6% (Table 2). The number of annual rings varied greatly (average 67.9 (s.d. 8.5) with a range of 43 to 88 years) among individuals and showed a positive correlation ($r$ = 0.65, $P$ < 0.01, Figure 4) with BA based on the measurement of the randomly100 disk photographs.

In the SEM analysis, the path from TWI to GR was not significant, and the model without this path was adopted as the final model. The values of the model fit metrics were 0.98, 0.94, 0.94 and 0.07 for GFI, AGFI, CFI and RMSEA, respectively; they generally indicated statistically acceptable solutions. The model explained approximately 17% of the variance in the PFH ($R^2$ = 0.17, Figure 5) when all estimated direct and indirect effects were considered.

The most important among all direct effects on the PFH was the crown ratio (CR) (standardized coefficient −0.32: $P < 0.01$, Table 3 and Figure 5). Furthermore, the direct effect of the number of branch scars (NBS) on PFH was significantly positive (0.13, $P < 0.01$, Table 3 and Figure 5). The indirect effect of CR on PFH via NBS was significantly negative (−0.04, $P < 0.01$, Figure 5). The total effect of CR was −0.36 ($P < 0.01$, Table 5 and Figure 5). The effects of individual size (BA) and the amounts of neighboring trees (BAS) on CR and NBS were both significant (BAS to CR was negative).

For the effect of BA on PFH, the direct effect was 0.19 ($P < 0.01$, Table 3 and Figure 5), and the indirect effect including all significant paths was −0.06 ($P < 0.05$, Table 4), with the direct effect exceeding the indirect effect. The total effect of BA was significantly positive (0.13, $P < 0.01$, Table 5). The effect of BAS on PFH was expressed as an indirect effect of paths through CR or NBS and through both factors, with the total effect being significantly positive (0.06, $P < 0.01$, Table 4). The direct effect of growth rate (GR) on PFH was not significant (−0.06, $P = 0.17$, Table 3 and Figure 5). The direct effect of TWI on PFH was significantly negative (−0.14, $P < 0.01$, Table 3 and Figure 5).

The percentage of trees with decay was 12.0% (58/482 trees), and 87.9% (51 trees) of them had false heartwood. The percentage was not significantly different ($P > 0.1$) from the percentage of false heartwood in all trees (80.3%). In contrast, the percentage of decay occurrence in each PFH class was significantly greater for PFH ≥ 21% than for PFH = 0% and 1-10% ($P < 0.05$, Figure 6).

Regarding the vertical distribution, PFHV was 12.4 (s.d. 11.9) % on average (range 0-41.3%). The highest frequency was observed in the 11-20% class (Figure 7). The PFHV was strongly correlated with the PFH at the lower tree heights, with correlation coefficients between 0.98 to 0.99 for each tree height (i.e., stump, 1, 1.3, 2 and 3 m height). The relative tree height at which the mean PFH reached its maximum was 9.7%, which corresponded to 1.82 (s.d. 1.52) m in terms of actual height (Figure 8). The mean PFH above this height decreased gradually toward the lowest live branch, where false heartwood disappeared in almost all trees (31/32 trees), resulting in an overall vertical conical shape (Figure 8).

## Discussion

In this study, we conducted an integrated analysis of the factors that cause false heartwood, which is considered a defect when using Japanese white birch wood for commercial purposes. Additionally, we were able to clarify the relative importance of the various causal factors to PFH.

SEM analysis revealed that CR was the most influential factor on PFH (Table 3 to 5, and Figure 5). The direct effect of CR on PFH was negative, suggesting that trees with more developed crowns had smaller false heartwood. This result supported hypothesis 1 that PFH is negatively correlated with CR. It is generally believed that trees with higher CR have high vigor due to the presence of abundant canopy leaves (Waring et al., 1981). Previous studies have often assumed that the vigor of trees is important for false heartwood (Basham, 1991; Kohler, 2006; Wernsdörfer et al., 2006; Giroud et al., 2008; Drouin et al., 2009). Individuals with high vigor were regarded as less likely to form false heartwood because they can quickly recover from external damage that triggers false heartwood (Baral et al., 2013). CR also had a negative indirect effect on PFH through NBS (Table 4 and Figure 5). NBS had a positive direct effect on PFH (Table 3; supporting hypothesis 2 that PFH is positively correlated with NBS), which may be due to increased oxygen penetration into the wood enhanced by more fallen branches (Solomon and Shigo, 1976; Belleville et al., 2011; Havreljuk et al., 2013). As a result, the total effect of CR was the strongest among all the variables.

The significant direct effect of BA on PFH supported hypothesis 3 that PFH is positively correlated with BA (Table 3 and Figure 2). This may be explained by the fact that large trees are reaching an age (> 70 years old; Figure 4) close to the life span of this species (c.a. 100 years; Osumi, 2005). In addition, the positive influence in the path BA → NBS → PFH implied that larger-sized individuals (mostly older trees) tend to develop false heartwood as they experience more events, such as stem damage, that lead to false heartwood formation. The close relationship of PFH expansion with tree age was consistent in previous studies (Cambell and Davidson, 1941; Knoke, 2003; Giroud et al., 2008; Belleville et al., 2011; Havreljuk et al., 2013), although they did not support the claim that it is solely determined by age. On the other hand, the indirect effects of BA through CR had a negative impact on PFH, reflecting the fact that trees with larger BA occupied canopy space earlier and maintained higher CR. Although the positive influence of BA → NBS → PFH was hidden by the negative influence of BA → CR → PFH (i.e., the indirect effect of BA was negative: Table 4), the presence of the direct effect (BA → PFH) overcomes it, resulting in a positive total effect (Table 5).

In contrast, the effect of GR on PFH was negative but not significant, which did not support hypothesis 4 that PFH was negatively correlated with GR (Table 3 and Figure 5). As expected, GR had a significant positive effect on CR. In contrast, the effect on GR from BA was negative, contrary to the expectation that trees with larger BA would exhibit higher growth rates. In a crowded even-aged stand, especially on a slope, similar to this study site, there is likely to be constant and intense belowground competition (Takahashi et al., 2003; Ohno, 2011), in which larger trees are known to occasionally show reduced growth affected by a lack of water resources. Because the growth rate fluctuated due to such size-dependent incidents, it may not be representative of the tree vigor at this study site.

Most studies have reached a consensus that drying stress is one of the most important factors in the formation of false heartwood (Trendelenburg, 1939; Shigo, 1986; Kohler, 2006; Giroud et al., 2021). This study also found that the value of TWI, which indicates the topographic wetness of the site, had a significant negative effect on PFH, supporting hypothesis 5 (Table 3 and Figure 5). This result suggests that PFH was generally higher in trees growing on the upper slope, which tended to have a greater water deficit than those growing on the lower slope. The relative importance of the effect of the TWI follows that of the CR.

***Relationship with decay***

Although decay can occur in all trees, a possible link between decay and false heartwood has widely been suggested (Trendelenburg, 1939; Campbell and Davidson, 1941; Siegle, 1967; Shigo and Hillis, 1973; Basham, 1991; Arač et al., 2021). The results of this study also indicated that the decay incidence was significantly higher in trees with larger PFH (PFH ≥ 21%) than in individuals with no false heartwood (PFH = 0%) or with relatively small PFH (PFH = 1-10%). In contrast, there was no significant difference between the frequency of false heartwood in all study trees (80.3%) and in decayed trees (87.2%). These contrasting results make it difficult to answer hypothesis 6 that false heartwood is a direct cause of decay. According to Shigo and Hillis (1973), the formation of false heartwood progresses more rapidly than decay, and decay triggered by false heartwood is expected to occur with a time delay. Decay is considered to be formed by temporally and spatially complex processes that intricately involve wound conditions (position, frequency, and severity) (Wiedenbeck and Smith, 2019) and compartmentalization (Shigo and Hillis, 1973). Further investigations are needed to determine their causal relationship.

***Vertical distribution of false heartwood***

On average, PFH within the entire tree stem reached a maximum at 9.7% relative tree height, close to the value (9%) reported for paper birch (Giroud et al., 2008). In most trees (31/32 trees), false heartwood was no longer observed above the lowest live branch, suggesting that a crown strongly limits the vertical formation of false heartwood. This result supports hypothesis 7, consistent with many other studies (Basham, 1991; Wernsdörfer et al., 2006; Giroud et al., 2008; Belleville et al., 2011). Some studies conducted on several tree species have reported that false heartwood often exhibits a vertical spindle shape (in which the PFH is smaller at both relatively low and high tree height positions), and the shape changes with time (Hallaksela and Niemistö, 1998; Wernsdörfer et al., 2005; Giroud et al., 2008). In this study, the vertical false heartwood shape was conical on average (Figure 8), supporting hypothesis 8. The current study site, which was at the older stage (approximately 70 years old) for Japanese white birch, may already be in a more advanced stage of development of false heartwood (Wernsdörfer et al., 2006). In addition, PFHV was strongly correlated with PFH measured at relatively low tree height positions (height of stump, 1 m, 1.3 m, 2 m, and 3 m). In this type of old birch secondary stand, it may be possible to estimate the PFHV by observing the PFH at the lower height position, including the stump height.

***Implications for forest management***

In this study, false heartwood at stump height was found in 80.3% of 482 study trees (Table 2). We supposed that this high occurrence of false heartwood would result from the condition of this study site, a crowded stand established after field burning without any subsequent human interference, in a drought-prone location. Many of the secondary birch stands in Hokkaido are often abandoned and dense, similar to this study site. Therefore, when using wood from these secondary stands, it is necessary to keep in mind the possibility of a high occurrence of false heartwood.

BAS was negatively correlated with CR and positively correlated with NBS. This implied that reducing local crowding could lead to a more developed crown and fewer branch scars, both of which can reduce false heartwood. This strongly suggests that thinning, as a standard management for an even-aged stand, also contributes to the reduction of false heartwood; the silvicultural measure for growth promotion would be compatible with defect control in birch forestry. When developing secondary birch forests, it will be possible to increase the proportion of high-value timber in the future by leaving trees with high CR at the time of thinning (Baral et al., 2013). Furthermore, when considering the development of young secondary birch stands, a previous study recommended intense thinning (90% of the number of trees in the stand) to enhance individual growth (Sano and Shibuya, 2015). This could also lead to a reduction in false heartwood by reducing individual crowding to continuously maintain a high CR, although this may also result in the development of live knots. In addition, the contribution of a lower TWI to a lower PFH suggested that lower-slope sites are more favorable than upper-slope sites for reducing false heartwood. In upper-slope sites, it may be effective to increase thinning intensity to compensate for the negative effect of TWI (Kohler, 2006).

Despite a multitude of studies, we are still unable to provide a complete explanation for false heartwood (Hörnfeld et al., 2010). In this study, we determined the relative importance of the multiple factors on PFH, but the $R^2$ value of the final model was limited to 17%. The formation of false heartwood seems to be more complex, including the presence of unknown factors. Therefore, to build a more explanatory model, factors not addressed in this study, such as damage to the stem and crown dieback (Giroud et al., 2021), should be examined in subsequent studies.

## Acknowledgments

We would like to thank the two anonymous reviewers and associate editor who devoted a great deal of time and effort to reviewing the manuscript. The reviewers' valuable comments and suggestions greatly improved the manuscript. We sincerely thank M. Kobayashi, K. Takagi, K. Uchiyama, H. Yamazaki, and members of the Uryu experimental forest for their support of this study. Thanks are extended to members of the Nayoro laboratory at Hokkaido University, Hokkaido Forest Products Research Institute and Hokkaido Forestry Research Institute.

## Competing interests statement

The authors declare that there are no competing interests.

## Author contribution statement

**AN:** Conceptualization; Data curation; Formal Analysis; Investigation; Methodology; Project administration; Software; Validation; Visualization; Writing – original draft. **HO:** Investigation; Writing – review & editing. **YO:** Investigation; Writing – review & editing. **TY:** Conceptualization; Funding acquisition; Investigation; Resources; Supervision; Writing – review & editing.


## Funding statement

This research was supported by JSPS KAKENHI (grant No. 20K06137).


## Data availability statement

Not currently available to the public.

## References


Aoyama, K., Yoshida, T., and Kamitani, T. 2009. An alternative of soil scarification treatment for forest restoration: effects of soil replacement. J. For. Res. **14**(1): 58–62. Doi:10.1007/s10310-008-0105-5.

Arač, K., Orlović, J.K., and Diminić, D. 2021. Effect of fungus Meripilus giganteus (Pers.) P. Karst. On occurrence and development of false heartwood and rot in Fagus sylvatica L. round wood. Croat. J. For. Eng. **42**(3): 529–542. Doi:10.5552/crojfe.2021.885.

Baral, S.K., Schneider, R., Pothier, D., and Berninger, F. 2013. Predicting sugar maple (Acer saccharum) discoloured wood characteristics. Can. J. For. Res. **43**(7): 649–657. Doi:10.1139/cjfr-2013-0017.

Basham, J.T. 1991. Stem decay in living trees in Ontario’s forests: a user’s compendium and guide. Forestry Canada, Ontario Region, Sault Ste. Marie, Ontario, Information Report O-X-408.

Belleville, B., Cloutier, A., and Achim, A. 2011. Detection of red heartwood in paper birch (*Betula papyrifera*) using external stem characteristics. Can. J. For. Res. **41**(7): 1491–1499. Doi:10.1139/x11-080.

Beven, K.J., and Kirkby, M.J. 1979. A physically based, variable contributing area model of basin hydrology. Hydrol. Sci. Bull. **24**(1): 43–69. Doi:10.1080/02626667909491834.

Campbell, W.A., and Davidson, R.W. 1941. Red heart of paper birch. J. For. **39**(1): 63–65. Doi:10.1093/jof/39.1.63.

Chi, X., Tang, Z., Xie, Z., Guo, Q., Zhang, M., Ge, J., Xiong, G., and Fang, J. 2015. Effects of size, neighbors, and site condition on tree growth in a subtropical evergreen and deciduous broad-leaved mixed forest, China. Ecol. Evol. **5**(22): 5149–5161. Doi:10.1002/ece3.1665.

Drouin, M., Beauregard, R., and Duchesne, I. 2009. Variability of wood color in paper birch in Quebec. Wood Fiber Sci. **41**(4): 333–345.

Giroud, G., Cloutier, A., and Alteyrac, J.M. 2008. Occurrence, proportion, and vertical distribution of red heartwood in paper birch. Can. J. For. Res. **38**(7): 1996–2002. Doi:10.1139/X08-043.

Giroud, G., Duchateau, E., Auger, I., Havreljuk, F., and Barrette, J. 2021. Regional variation in wood discoloration in paper birch trees. Can. J. For. Res. **51**(10): 1512–1520. Doi:10.1139/cjfr-2020-0475.

Hallaksela, A.M., and Niemistö, P. 1998. Stem discoloration of planted silver birch. Scand. J. For. Res. **13**(1-4): 169–176. Doi:10.1080/02827589809382973.

Hasenauer, H., and Monserud, R.A. 1996. A crown ratio model for Austrian forests. For. Ecol. Manag. **84**(1): 49–60. Doi:10.1016/0378-1127(96)03768-1.

Havreljuk, F., Achim, A., and Pothier, D. 2013. Regional variation in the proportion of red heartwood in sugar maple and yellow birch. Can. J. For. Res. **43**(3): 278–287. Doi:10.1139/cjfr-2012-0479.

Hemery, G.E., Savill, P.S., and Pryor, S.N. 2005. Applications of the crown diameter–stem diameter relationship for different species of broadleaved trees. For. Ecol. Manag. **215**(1): 285–294. Doi:10.1016/j.foreco.2005.05.016.

Hofmann, T., Guran, R., Zitka, O., Visi-Rajczi, E., and Albert, L. 2022. Liquid chromatographic/mass spectrometric study on the role of beech (Fagus sylvatica L.) wood polyphenols in red heartwood formation. Forests **13**(1): 10. Doi:10.3390/f13010010.

Hörnfeldt, R., Drouin, M., and Woxblom, L. 2010. False heartwood in beech Fagus sylvatica, birch *Betula pendula*, *B. papyrifera* and ash *Fraxinus excelsior* – an overview. Ecol.

Bull. **53**: 61–76.

Jönsson, M.T., Fraver, S., Jonsson, B.G., Dynesius, M., Rydgård, M., and Esseen, P.A. 2007. Eighteen years of tree mortality and structural change in an experimentally fragmented Norway spruce forest. For. Ecol. Manag. **242**(2): 306–313. Doi:10.1016/j.foreco.2007.01.048.

Knoke, T. 2003. Predicting red heartwood formation in beech trees (Fagus sylvatica L.). Ecol. Model. **169**(2): 295–312. Doi:10.1016/S0304-3800(03)00276-X.

Knoke, T., and Wenderoth, S.S. 2001. Ein ansatz zur beschreibung von wahrscheinlichkeit und ausmaß der farbkernbildung bei buche (Fagus sylvatica L.). forstwiss. Cent. Ver. Mit Tharandter Forstl. Jahrb. **120**(1): 154–172. Doi:10.1007/BF02796089.

Koch, G. 2004. Eigenheiten des rotkerniges buchenholzesed. Bundesforschungsanstalt für Forst- und Holzwirtschaft, Hamburg, German.

Kohler, H. 2006. Die farbverkernungssysteme der rotbucheed. Schwaigern Selbstverlag, Schwaigern, Germany.

Lam, T.Y., and Maguire, D.A. 2012. Structural equation modeling: theory and applications in forest management. Int. J. For. Res. **2012**: 263953. Doi:10.1155/2012/263953.

Laughlin, D.C., and Fulé, P.Z. 2008. Wildland fire effects on understory plant communities in two fire-prone forests. Can. J. For. Res. **38**(1): 133–142. Doi:10.1139/X07-118.

Ohno, Y. 2011. Clarification of factors contributing to crown dieback of *Betula maximowicziana* canopy trees in deciduous broad-leaved forests. Bull. Hokkaido For. Res. Inst. **48**: 1–46.

Osumi, K. 2005. Reciprocal distribution of two congeneric trees, Betula platyphylla var. japonica and Betula maximowicziana, in a landscape dominated by anthropogenic disturbances in northeastern Japan. J. Biogeogr. **32**(12): 2057–2068. Doi:10.1111/j.1365-2699.2005.01368.x.

Pape, R. 2002. Red heart in birch – origin, properties and utilization. Rep. No. 2.

Pastur, G.M., Lencinas, M.V., Cellini, J.M., and Mundo, I. 2007. Diameter growth: can live trees decrease? Forestry **80**(1): 83–88. Doi:10.1093/forestry/cpl047.

QGIS Development Team. 2021. QGIS geographic information system. Open source geospatial foundation project. https://www.qgis.org/ja/site/

R Development Core Team. 2022. R: a language and environment for statistical computing. R Foundation for Statistical Computing. Available from https://www.R-project.org/[accessed 6 June 2022].

Račko, V., and Čunderlík, I. 2002. Influence of some factors on beech false heartwood formation 1. Influence of tree age, ripewood ratio and stem diameter. Wood Res. **47**(2): 7–17.

Račko, V., and Čunderlík, I. 2010. Which of the factors do significantly affect beech false heartwood formation?, ***In*** Hardwood science and technology, the $4^{\text{th}}$ conference on hardwood research and utilization in Europe. University of Sopron, Hungary, Europe. Pp. 94–95.

Razali, N.M., and Wah, Y.B. 2011. Power comparisons of Shapiro-Wilk, Kolmogorov-Smirnov, Lilliefors and Anderson-Darling tests. J. Stat. Model. Anal. **2**(1): 21–33.

Rosseel, Y. 2012. Lavaan: an R package for structural equation modeling. J. Stat. Softw. **48**: 1–36. Doi:10.18637/jss.v048.i02.

Sano, Y., Shibuya, M. 2015. Thinning effect on tree growth in secondary *Betula ermanii* stands on scarified sites. J. Jpn. For. Soc. **97**: 25–29.

Schneider, C.A., Rasband, W.S., and Eliceiri, K.W. 2012. NIH Image to ImageJ: 25 years of image analysis. Nat. Methods **9**(7): 671–675. Doi:10.1038/nmeth.2089.

Shigo, A.L. 1984. Compartmentalization: A conceptual framework for understanding how trees grow and defend themselves. Annu. Rev. Phytopathol. **22**: 189–214. Doi.org/10.1146/annurev.py.22.090184.001201.

Shigo, A.L. 1986. A new tree biology dictionary. Shigo and Trees, Associates, Durham, NH.

Shigo, A.L., and Hillis, W.E. 1973. Heartwood, discolored wood, and microorganisms in living trees. Annu. Rev. Phytopathol. **11**(1): 197–222. Doi:10.1146/annurev.py.11.090173.001213.

Shimase, T. 2021. Status and prospects of locally grown birch (Betula sp.) wood demand in Hokkaido, Japan. Boreal For. Res. **69**: 35–37.

Siegle, H. 1967. Microbiological and biochemical aspects of heartwood stain in *Betula papyrifera* Marsh. Can. J. Bot. **45**(2): 147–154. Doi:10.1139/b67-011.

Solomon, D, S., and Shigo, A, L. 1976. Discoloration and decay associated with pruning wounds on yellow birch. Forest Science. **22**(4): 391–392. Doi.org/10.1093/forestscience/22.4.391.

Takahashi, K., Uemura, S., Suzuki, J.I., and Hara, T. 2003. Effects of understory dwarf bamboo on soil water and the growth of overstory trees in a dense secondary Betula ermanii forest, northern Japan. Ecol. Res. **18**(6): 767–774. Doi:10.1007/s11284-003-0594-9.

Trendelenburg, R. 1939. Das holz als rohstoffed. Lehmanns Verlag, Munich, Germany.

Venet, J. 1986. Identification et classement des bois françaised. École Nationale du Génie Rurale, des Eaux et des Forêts, Nancy, France.

Waring, R.H., Newman, K.E.N., and Bell, J. 1981. Efficiency of tree crowns and stemwood production at different canopy leaf densities. For. Int. J. For. Res. **54**(2): 129–137. Doi:10.1093/forestry/54.2.129.

Wernsdörfer, H., Constant, T., Mothe, F., Badia, M.A., Nepveu, G., and Seeling, U. 2005. Detailed analysis of the geometric relationship between external traits and the shape of red heartwood in beech trees (Fagus sylvatica L.). Trees **19**(4): 482–491. Doi:10.1007/s00468-005-0410-y.

Wernsdörfer, H., Le Moguédec, G., Constant, T., Mothe, F., Nepveu, G., and Seeling, U. 2006. Modelling of the shape of red heartwood in beech trees (Fagus sylvatica L.) based on external tree characteristics. Ann. For. Sci. **63**(8): 905–913. Doi:10.1051/forest:2006074.

Wiedenbeck, J., Smith, K, T. 2019. Hardwood management, tree wound response, and wood product value. The Forestry Chronicle. **94**(3): 292-306.

Yamazaki, H., and Yoshida, T. 2018. Significance and limitation of scarification treatments on early establishment of Betula maximowicziana, a tree species producing buried seeds: effects of surface soil retention. J. For. Res. **23**(3): 166–172. Doi:10.1080/13416979.2018.1452458.

## Tables

**Table 1.** Tree species composition of the study stand in a secondary forest.

| Species | **Density ($stems \cdot h^{-1}$)** | **Volume ($m^3 \cdot ha^{-1}$)** | **Basal area ($m^2 \cdot ha^{-1}$)** | **Mean DBH and standard deviation (cm)** |
|---|---|---|---|---|
| *Betula platyphylla* var. *japonica* | 352 | 116.0 | 15.7 | 23.0 ± 6.3 |
| *Quercus crispula* | 54 | 20.6 | 2.5 | 23.4 ± 7.4 |
| *Betula ermanii* | 26 | 6.1 | 0.9 | 19.6 ± 5.5 |
| *Abies sachalinensis* | 17 | 5.5 | 0.7 | 21.1 ± 7.9 |
| Others | 96 | 21.0 | 2.9 | 19.0 ± 5.7 |
| Total | 546 | 169.1 | 22.7 | 22.1 ± 6.5 |

Others include *Acer pictum* Thunb., *Phellodendron amurense* var. *amurense*, *Alnus hirsute* Turcz. Var. *hirsute.*, etc.

**Table 2.** Mean, standard deviation and range of the observed variables for *B. platyphylla* var. *japonica* tree individuals.

| Observed variable | **Description** | **Mean and standard deviation** | **Range** |
|---|---|---|---|
| PFH (%) | The proportion of false heartwood area to the disk surface area (excluding the bark) | 16.4 ± 14.0 | 0.0-63.6 |
| BA ($m^2$) | Individual basal area calculated from DBH | 0.04 ± 0.02 | 0.01-0.15 |
| GR (%) | Individual growth rate for the last 10 years | 14.1 ± 4.6 | 5.1-32.4 |
| CR (%) | Ratio of crown length to tree height | 24.9 ± 10.1 | 10.0-50.0 |
| NBS | Number of branch scars with width more than 1/3 of the stem diameter at the height | 23.7 ± 9.8 | 0.0-64.0 |
| BAS ($m^2$) | Basal area sum of neighboring (within 5 m radius) trees | 0.23 ± 0.10 | 0.02-0.54 |
| TWI | Topographic wetness index at the scale of 400 $m^2$ | 7.2 ± 0.6 | 5.2-8.7 |

**Table 3.** Estimated direct effects of the structural equation modeling, along with corresponding standard errors, *Z* values and *P* values (see Figure 5). (PFH: The proportion of false heartwood, BA: Basal area, GR: Growth rate, CR: Crown ratio, NBS: Number of branch scars, BAS: Basal area sum of neighboring trees, TWI: Topographic wetness index)

| Path model | **Direct effect** | **Standard error** | **Standardized coefficients** | ***Z* value** | ***P* value** |
|---|---|---|---|---|---|
| PFH = | | | | | |
| BA | 110.947 | 28.067 | 0.19 | 3.953 | 0.000 |
| GR | −0.173 | 0.127 | −0.06 | −1.362 | 0.173 |
| CR | −0.435 | 0.063 | −0.32 | −6.875 | 0.000 |
| NBS | 0.194 | 0.064 | 0.13 | 3.023 | 0.003 |
| TWI | −3.222 | 0.974 | −0.14 | −3.307 | 0.001 |
| GR = | | | | | |
| BA | −34.517 | 9.375 | −0.18 | −3.682 | 0.000 |
| CR | 0.054 | 0.022 | 0.12 | 2.474 | 0.013 |
| BAS | 0.371 | 2.182 | 0.01 | 0.170 | 0.865 |
| CR = | | | | | |
| BA | 138.477 | 18.550 | 0.32 | 7.465 | 0.000 |
| BAS | −12.131 | 4.526 | −0.12 | −2.680 | 0.007 |
| NBS = | | | | | |
| BA | 149.974 | 18.428 | 0.36 | 8.139 | 0.000 |
| CR | −0.274 | 0.043 | −0.28 | −6.398 | 0.000 |
| BAS | 9.947 | 4.289 | 0.10 | 2.319 | 0.020 |

**Table 4.** Estimated combined indirect effects of the structural equation modeling, along with corresponding standard errors, *Z* values and *P* values (see Figure 5). (PFH: The proportion of false heartwood, BA: Basal area, CR: Crown ratio, BAS: Basal area sum of neighboring trees)

| Path model | **Indirect effect** | **Standard error** | **Standardized coefficients** | ***Z* value** | ***P* value** |
|---|---|---|---|---|---|
| PFH = | | | | | |
| BA | −33.860 | 16.790 | −0.06 | −2.017 | 0.044 |
| CR | −0.062 | 0.021 | −0.04 | −2.980 | 0.003 |
| BAS | 7.897 | 2.611 | −0.02 | 3.024 | 0.002 |

**Table 5.** Estimated total effects (i.e., direct path and all possible indirect paths) of the structural equation modeling, along with corresponding standard errors, *Z* values and *P* values (see Figure 5). (PFH: proportion of false heartwood, BA: basal area, CR: crown ratio)

| Path model | **Total effect** | **Standard error** | **Standardized coefficients** | ***Z* value** | ***P* value** |
|---|---|---|---|---|---|
| PFH = | | | | | |
| BA | 77.088 | 26.699 | 0.13 | 2.887 | 0.004 |
| CR | −0.497 | 0.061 | −0.36 | −8.172 | 0.000 |

**Figure captions**

**Figure 1.** The mustache-patterned branch scar that characterizes birch. Scars with a width greater than 1/3 of the stem at height were targeted in this study.

**Figure 2.** Hypothetical model to explain the proportion of false heartwood (PFH). The direct or indirect pathways for each factor on PFH are shown. Signs (+ or −) indicate expected directions of relationships. BA: basal area, GR: growth rate, CR: crown ratio, NBS: number of branch scars, BAS: basal area sum of neighboring trees, TWI: topographic wetness index.

**Figure 3.** Frequency distribution of the proportion of false heartwood for *Betula platyphylla* var. *japonica* ($n$ = 482) in the study stand.

**Figure 4.** Relationship between tree basal area ($m^2$) and tree age (years) in 100 randomly selected trees. The regression line represents the relationship between basal area and age. The circle size corresponds to the proportion of false heartwood (max = 50.5%, min = 0%).

**Figure 5.** Structural equation modeling (Goodness-of-fit index: GFI = 0.985, AGFI = 0.942, CFI = 0.943, RMEA = 0.066) with standardized parameter estimates. The error arrows of the observed variables are omitted to simplify the diagram. Estimated standardized path coefficients (direct effects) are placed on each path. The squared multiple correlations ($R^2$)

are included for each endogenous latent variable. The thickness of a single arrowhead corresponds to the magnitude of its estimates. The dashed single arrowheads depict nonsignificant paths. The double arrowheads depict the error covariance between the errors of BA (basal area) and BAS (basal area sum of neighboring trees) latent variables. PFH: proportion of false heartwood, GR: growth rate, CR: crown ratio, NBS: number of branch scars, TWI: topographic wetness index.

**Figure 6.** Percentage with decay by proportion of false heartwood ($n$ = 482). Due to the sample size, “the proportion of false heartwood (PFH) ≥ 21%” was combined into one group (PFH = 0: 97, 1-10%: 168, 11-20%: 99, ≥ 21%: 118 individuals). The legend indicates the percentage of decay rate included in each PFH. The different letters indicate significant differences at $P < 0.05$ in the Tukey test.

**Figure 7.** Frequency distribution of the proportion of false heartwood volume to the entire stem volume (PFHV) for *Betula platyphylla* var. *japonica* ($n$ = 32) in the study stand.

**Figure 8.** Distribution of the proportion of false heartwood (PFH) along relative tree height. The PFH at each height of 32 trees are pooled and shown. The dashed line indicates the mean relative height of the lowest live branch. The squares indicate the mean PFH of relative

height classes of approximately 5, 10, 20, 30, 40, 50, 60, and 70%.

**Figures**

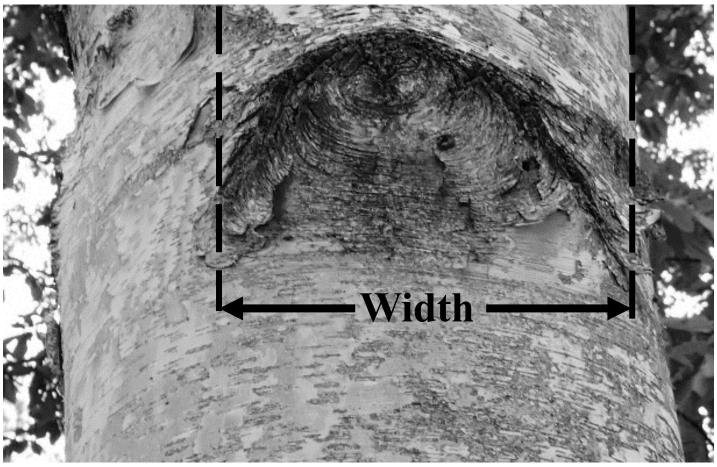


**Figure 1.** The mustache-patterned branch scar that characterizes birch. Scars with a width greater than 1/3 of the stem at height were targeted in this study.

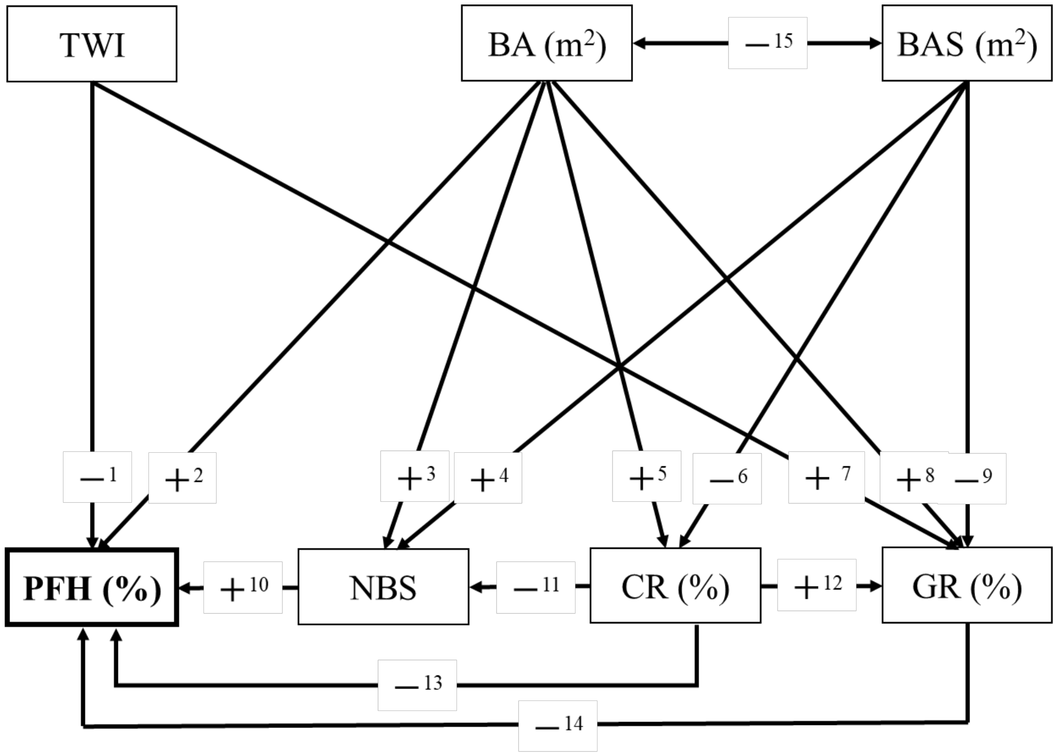


**Figure 2.** Hypothetical model to explain the proportion of false heartwood (PFH). The direct or indirect pathways for each factor on PFH are shown. Signs (+ or −) indicate expected directions of relationships. BA: basal area, GR: growth rate, CR: crown ratio, NBS: number of branch scars, BAS: basal area sum of neighboring trees, TWI: topographic wetness index.

---

The numbers assigned to each path correspond to the literature on which they are based.

[1] Trendelenburg, 1939; Shigo, 1986; Kohler,2006; Giroud et al., 2021.
[2] Hallaksela and Niemistö, 1998; Knoke, 2003; Giroud et al., 2008; Belleville et al., 2011.
[3] Knoke, 2003; Wernsdörfer et al.,2005.
[4] Knoke, 2003.
[5] Hemery et al., 2005.
[6] Knoke, 2003.
[7] Pastur et al., 2007.
[8] Chi et al., 2015.
[9] Knoke, 2003; Chi et al., 2015.
[10] Knoke, 2003; Wernsdörfer et al., 2005; Giroud et al., 2008; Belleville et al., 2011.
[11] Knoke, 2003.
[12] Hasenauer and Monserud, 1996.
[13] Basham, 1991; Giroud et al., 2008; Drouin et al., 2009.
[14] Wernsdörfer et al., 2006; Baral et al., 2013.
[15] Jönsson et al., 2007.

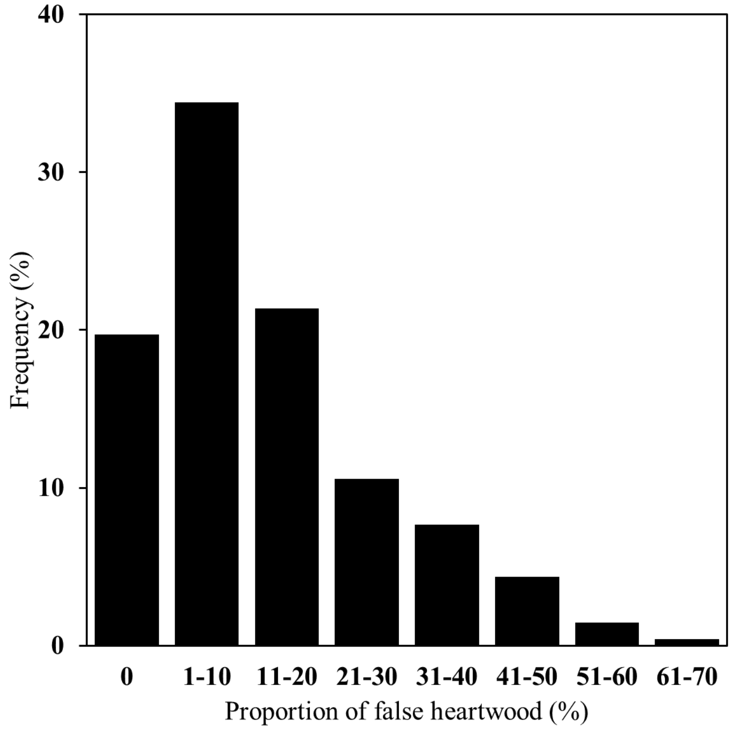


**Figure 3.** Frequency distribution of the proportion of false heartwood for *Betula platyphylla* var. *japonica* ($n$ = 482) in the study stand.

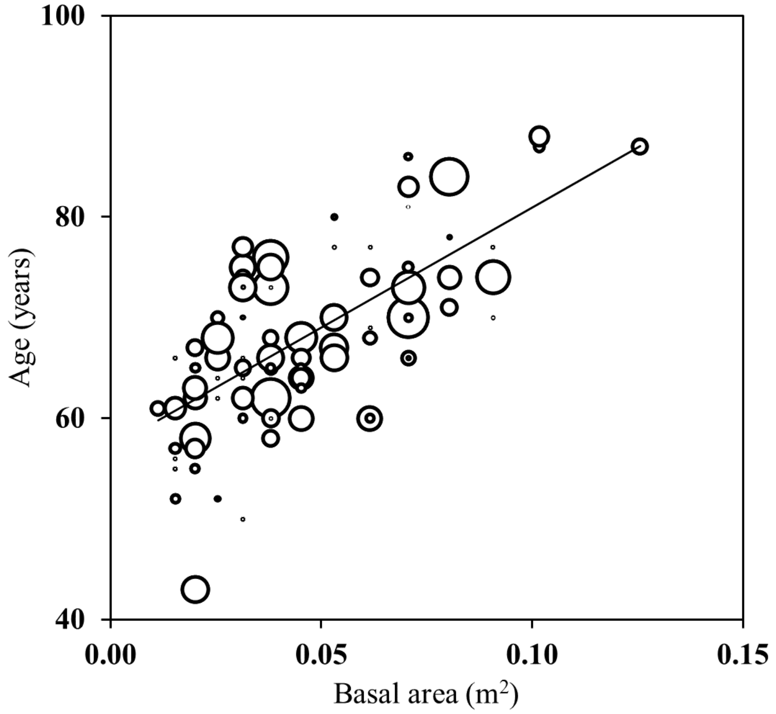


**Figure 4.** Relationship between tree basal area ($m^2$) and tree age (years) in 100 randomly selected trees. The regression line represents the relationship between basal area and age. The circle size corresponds to the proportion of false heartwood (max = 50.5%, min = 0%).

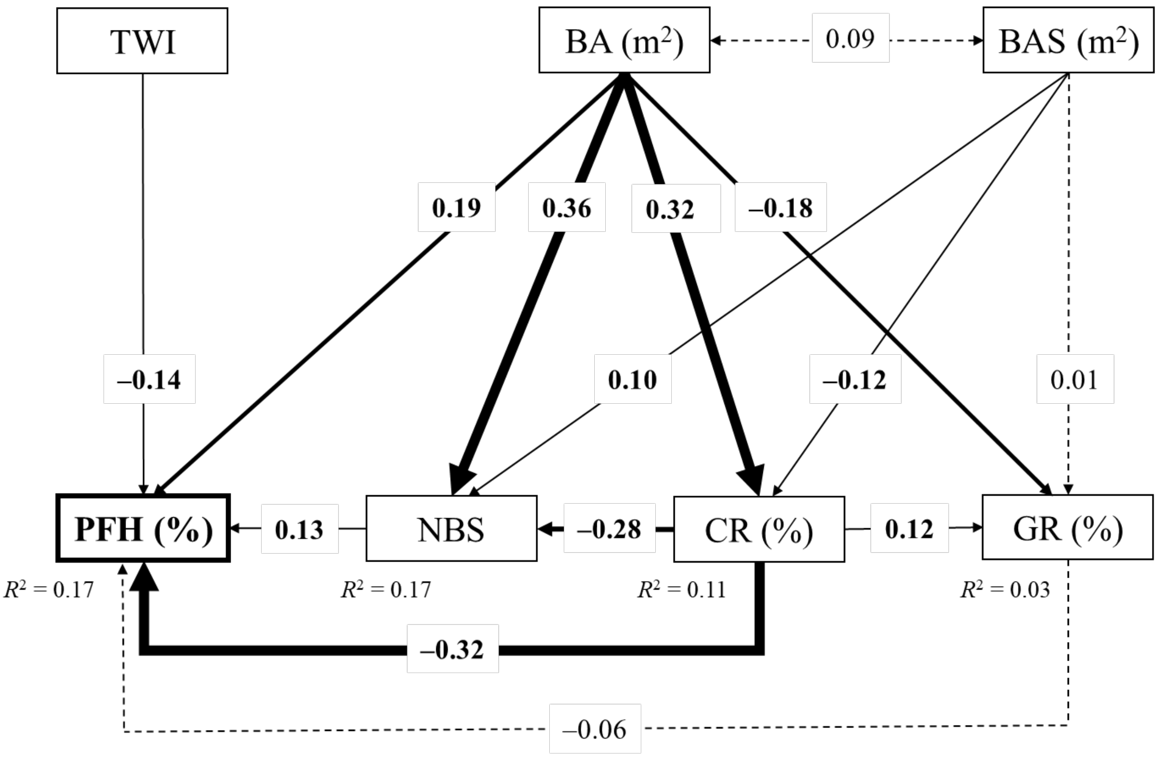


**Figure 5.** Structural equation modeling (Goodness-of-fit index: GFI = 0.985, AGFI = 0.942, CFI = 0.943, RMEA = 0.066) with standardized parameter estimates. The error arrows of the observed variables are omitted to simplify the diagram. Estimated standardized path coefficients (direct effects) are placed on each path. The squared multiple correlations ($R^2$) are included for each endogenous latent variable. The thickness of a single arrowhead corresponds to the magnitude of its estimates. The dashed single arrowheads depict nonsignificant paths. The double arrowheads depict the error covariance between the errors of BA (basal area) and BAS (basal area sum of neighboring trees) latent variables. PFH: proportion of false heartwood, GR: growth rate, CR: crown ratio, NBS: number of branch

scars, TWI: topographic wetness index.

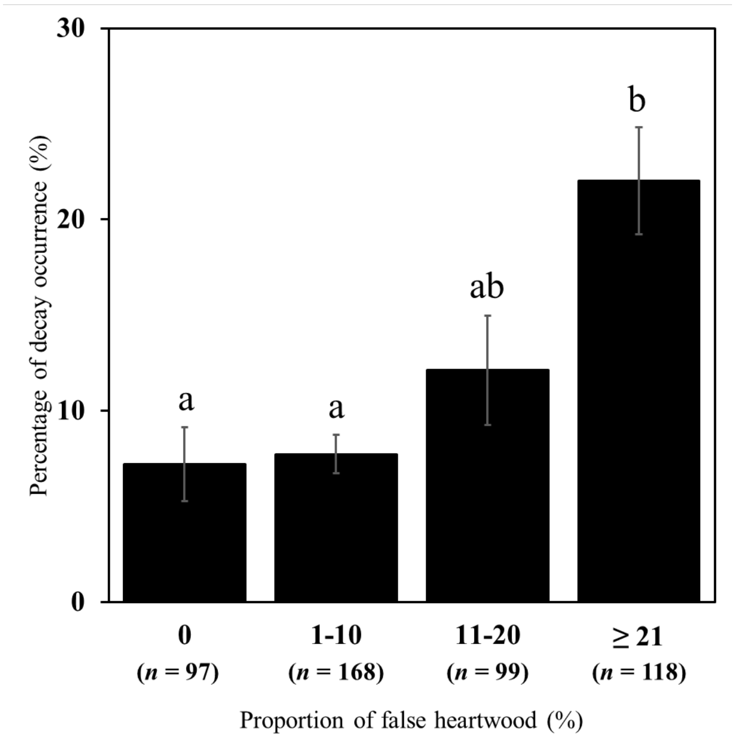


**Figure 6.** Percentage with decay by the proportion of false heartwood (*n* = 482). The legend indicates the percentage of decay rate included in each PFH. The different letters indicate significant differences at $P < 0.05$ in the Tukey test.

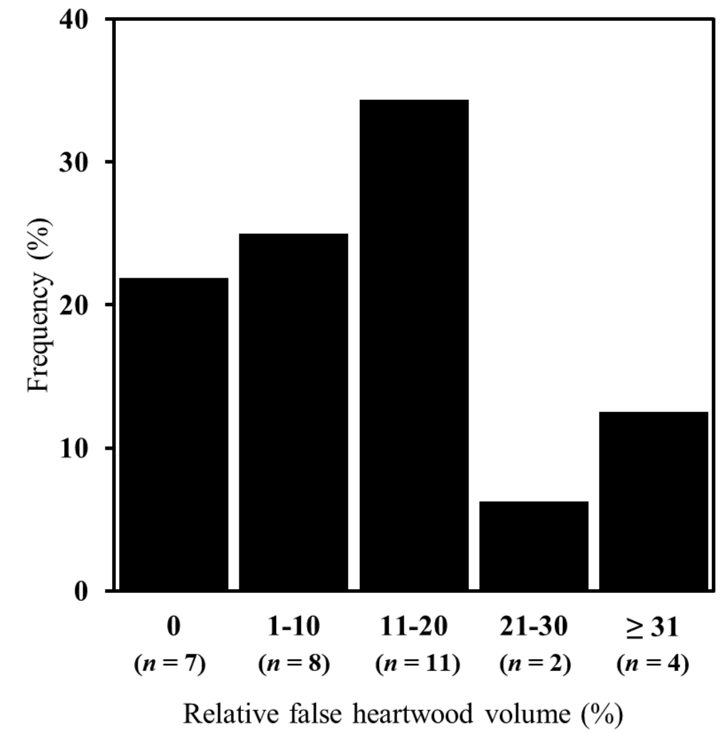


**Figure 7.** Frequency distribution of the proportion of false heartwood volume to the entire stem volume for *Betula platyphylla* var. *japonica* ($n$ = 32) in the study stand.

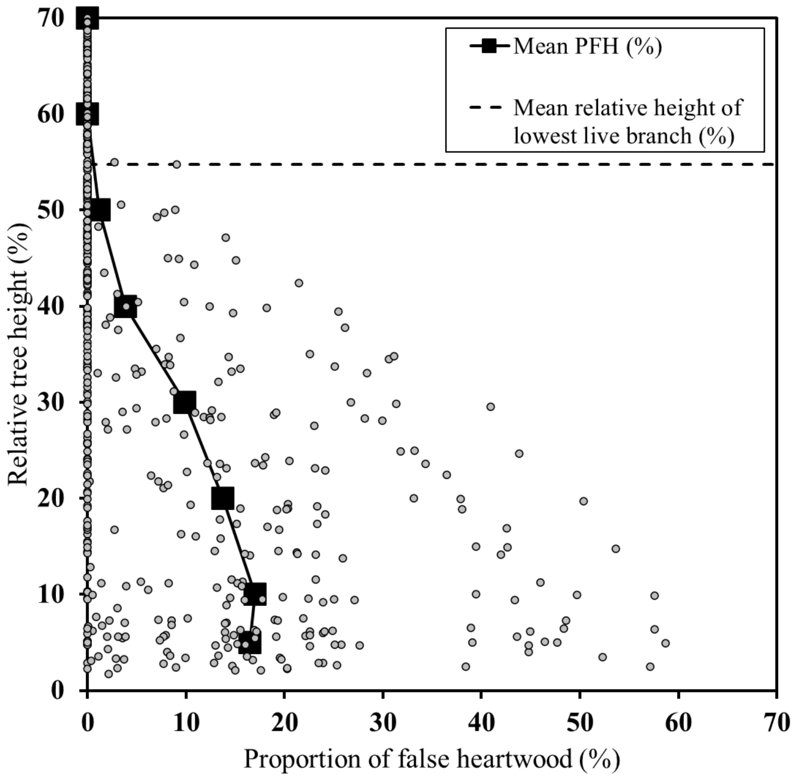


**Figure 8.** Distribution of the proportion of false heartwood (PFH) along relative tree height. The PFH at each height of 32 trees are pooled and shown. The dashed line indicates the mean relative height of the lowest live branch. The squares indicate the mean PFH of relative height classes approximately 5, 10, 20, 30, 40, 50, 60, and 70%.